# Creep Behavior of an Oxide Dispersion Strengthened Iron with Ultrafine Grain Structure

V. Dudko[1,a], R. Kaibyshev[1,b], A. Belyakov[1,c], Y. Sakai[2,d], K. Tsuzaki[3,e]

[1]Belgorod State University, Pobedy 85, Belgorod 308015, Russia

[2]Innovative Materials Engineering Laboratory, Nationals Research Institute for Metals, Sengen 1-2-1, Tsukuba, Ibaraki 305-0047, Japan

[3]Structural Metals Center, Nationals Research Institute for Metals, Sengen 1-2-1, Tsukuba, Ibaraki 305-0047, Japan

[a]valeriy_dudko@yahoo.com, [b]rustam_Kaibyshev@bsu.edu.ru, [c]belyakov@bsu.edu.ru, [d]sakai.yoshikazu@nims.go.jp, [e]tsuzaki.kaneaki@nims.go.jp

**Keywords:** creep; oxide dispersion strengthening steel; threshold stress; deformation mechanisms.

**Abstract.** The creep behavior of oxide-bearing Fe-0.6%O steel was studied in the temperature range of 550-700°C at stresses ranging from 100 to 400 MPa. The creep data showed high values of an apparent stress exponent n close to ~16 for power-law creep. In addition the apparent experimental activation energy was much higher than that for the lattice diffusion in α-iron. Analysis of creep data revealed that the deformation behavior was strongly affected by the threshold stresses, which are associated with the interaction between moving dislocations and fine incoherent oxide particles. Analysis of deformation behavior in terms of threshold stress leads the true stress exponent of ~8; the activation energy for creep became close to value of activation energy for lattice diffusion at 700°C and for pipe-diffusion in the temperature range of 550–650°C.

## Introduction

The creep resistance of high-temperature structural materials can be significantly improved by an incorporation into metallic matrix various incoherent and non-shearable oxide particles by using different powder metallurgy techniques. One of them is mechanical milling followed by consolidating plastic working [1, 2]. This processing method allows us to develop products with commercial dimensions using almost unlimited variety of materials. This technique was recently applied for the fabrication of the high-strength steels with ultrafine grain structure containing nano-scale oxides, which are homogeneously dispersed throughout the ferrite matrix [3].

The relationship between the steady state strain rate, $\dot{\varepsilon}$, and the flow stresses, σ, at elevated temperatures is generally represented as follows [4, 5]:

$$\dot{\varepsilon} = A\sigma^{n} \exp\left(\frac{-Q}{RT}\right), \tag{1}$$

where $A$ and $n$ are constants, $Q$ is the activation energy for plastic deformation, $R$ is the gas constant and $T$ is the absolute temperature. The value of stress exponent, $n$, varies from 3 to 7, depending on operating mechanisms of dislocation motion. Correspondingly, the experimental value of activation energy matches the activation energies for lattice self-diffusion, pipe diffusion or grain boundary diffusion. However, mechanisms of plastic flow at relative low deformation temperatures have not been studied in sufficient detail. Especially that concerns oxide dispersion strengthening (ODS) materials, which were investigated at high homological temperatures [6, 7]. Moreover, the most of studies were focused on the deformation behavior of materials with face-centered cubic lattice, while the deformation mechanisms of ODS alloys with body-centered cubic lattice were not clarified.

The aim of the present work was to study the deformation mechanisms in a pure iron containing about 2 volume pct of $Fe_3O_4$ oxides with an average size of ~10 nm [3] in the temperature range of 550-700°C. A careful analysis of the creep behavior in terms of threshold stresses was carried out. Microstructure observations were focused on the interaction mechanisms between lattice dislocations and the nanoscale oxides.

## Experimental

An Fe–0.6%O steel (0.58%O, 1.2%Cr, 0.5%Ni, 0.18%Mn:, 0.11%W, 0.11%Si, 0.05%Cu, 0.01%C, 0.009%P, 0.007%S, all in weight %, the balance Fe) was used as the starting material. The $Fe_3O_4$ oxide particles with an average size of about 10 nm comprised about 2% as volume fraction. The processing method consisting of mechanical milling followed by consolidating plastic working was detailed elsewhere [3]. The samples were annealed at a temperature of 810°C for 25 h. The final average grain size in the annealed samples was about 500 nm; and the oxide particles were homogeneously distributed in the matrix with an average interparticle spacing of about 200 nm. The creep/compression tests were carried out in the temperature range 550-700°C. The creep tests were carried out in constant stress creep testing machine at strain rates ranging from $10^{-8}$ to $10^{-5}$ $s^{-1}$. The compression tests were carried out at constant initial strain rates ranging from $1.4 \times 10^{-6}$ to $10^{-2}$ $s^{-1}$ by using a Schenk RMS100 universal testing machine. The specimens of Ø4 mm and 20 mm in gauge length and Ø7 mm and 11 mm in height were machined from bulk rods for creep and compression tests, respectively. The specimens were covered by the aluminum and boron oxide powders to prevent oxidation. The structural analysis was carried out using a Jeol JEM-2000E transmission electron microscope (TEM). The TEM foils were electropolished by using a Tenupol 3 twinjet polishing unit with an electrolyte containing 5% perchloric acid and 95% acetic acid at room temperature.

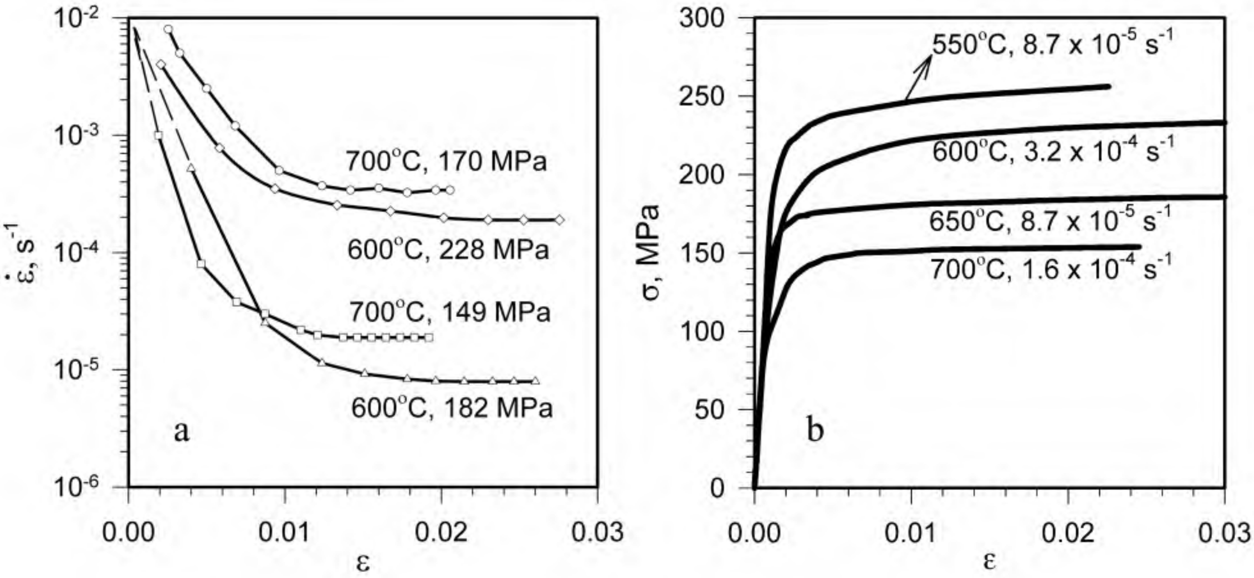

Figure 1. A series of the flow curves obtained during creep (a) and compression (b) tests of Fe – 0.6%O steel.

## Results

Typical flow curves for creep and compression tests are shown in Fig. 1. The creep/deformation behavior is characterized by a short transition stage followed by a steady state flow. Namely, the strain rate sharply decreases to its minimum value at strains below 0.012, and then becomes invariant over the subsequent deformation (Fig. 1a). Similarly, the flow stresses rapidly increase to their saturations, leading to a steady state flow. Assuming that the deformation/creep behavior obeys the power law relationship (1), unusually high values of stress exponent of above 16 were obtained from the experimental data taken at steady-state flow (Fig. 2a). It should also be noted that contrary to general creep behavior of various single-phase metallic materials [4, 5], the measured values of the stress exponent increase with decreasing the creep rate.

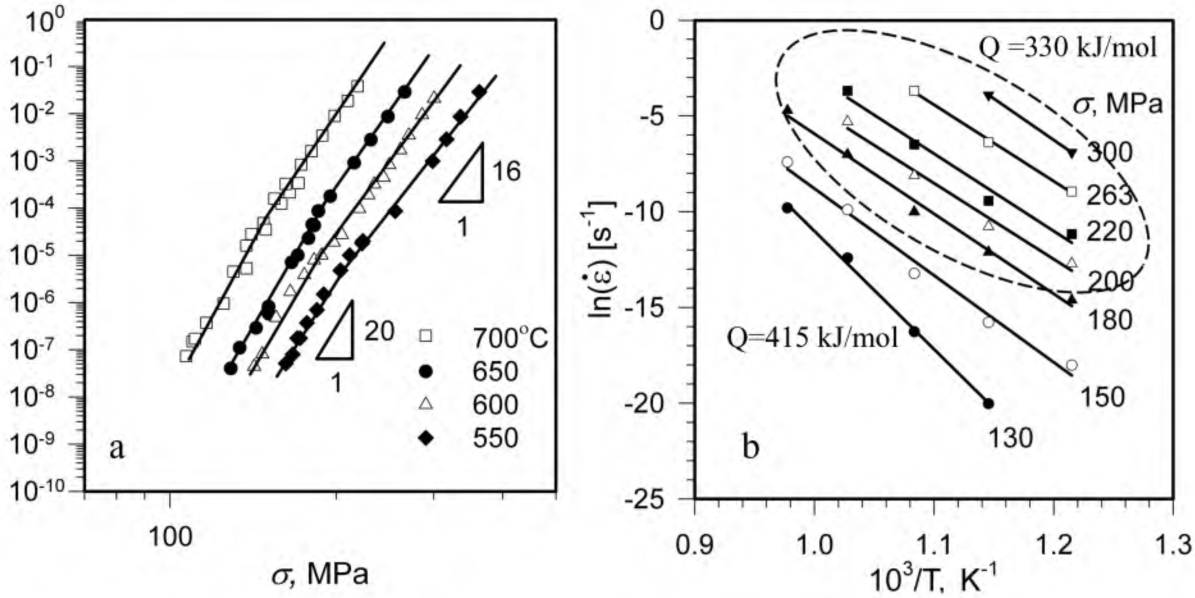

Fig. 2. Relationships between steady state strain rate and flow stress (a) and temperature (b) for Fe – 0.6%O steel.

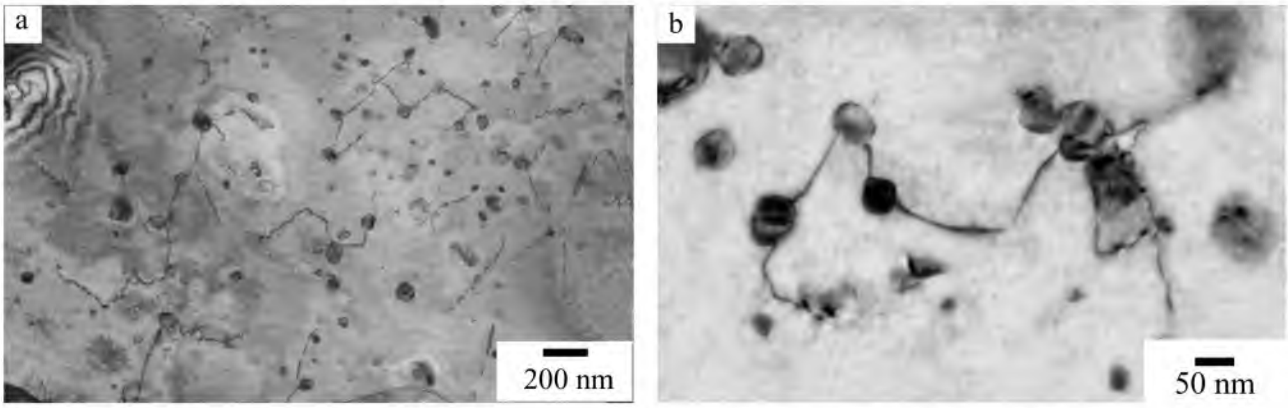

Figure 3. TEM micrographs showing the homogenous distribution of oxide particles (a), the interaction between dislocations and oxide particles (b) in Fe –- 0.6% O after creep at 600°C and $\dot{\varepsilon} = 1.3 \times 10^{-7}$ $s^{-1}$.

Fig. 2b shows the plot of the steady-state creep rates, $\dot{\varepsilon}$, against the inverse absolute temperature for different applied stress levels in semi-logarithmic scale. It is seen that the strain rate can be represented by a linear function of 1/T for each stress level. Therefore, the apparent activation energy for plastic deformation can be estimated from the slope of these straight lines. The estimated values of activation energy vary from 415 to 330 kJ/mol when the flow stresses increase from 130 to 300 MPa. A decrease in activation energy with increasing flow stress was frequently observed in hot deformation and creep of metals and alloys. However, the activation energies, which are more than one and half of the activation energy for self-diffusion ($Q_l$=251 kJ/mol [5]), and the high values of the stress exponents were obtained only for dispersion strengthened alloys.

The structural observations revealed an extensive interaction between lattice dislocations and nanoscale spherical particles with size ranging from 5 to 50 nm (Fig. 3). The particles act as effective obstacles for the dislocation motion. Highly curved configuration of lattice dislocations can be interpreted in terms of the local climb model [8, 9] or the detachment model [10]. It should be noted that the deformation temperature and the creep/strain rate do not have significant effect on the dislocation substructures. It is supposed, therefore, that the mechanism of interaction between dislocations and the oxide particles remains unchanged with temperature variation in range 550-700°.

## Discussion

Dispersion strengthened alloys are characterized by high creep resistance at elevated temperatures because of presence threshold stress, $\sigma_{th}$, below which the strain rate is assumed to be negligible [6, 7, 11]. To reveal deformation mechanisms operating in these alloys the deformation behavior of these materials is analyzed in terms of threshold stress [11]. In order to estimate the threshold stress, the experimental data were plotted as $\dot{\varepsilon}^{1/n}$ against $\sigma$ on a double linear scale for various possible *n* for each deformation temperature (*e.g.* Fig. 4). The values of *n*, which provide the best linear fit of $\dot{\varepsilon}^{1/n}$ *vs* $\sigma$, were considered as the true stress exponents. The threshold stresses obtained by the linear extrapolation to zero strain rate are presented in Table 1. The values of threshold stresses are sufficiently high and constitute the much of steady state flow stresses. Due to the presence of high threshold stress the ODS steel exhibits the same creep strength as modern creep resistant steels with martensitic structures. Therefore, the strengthening of steels by nanooxides can be considered as high-performance method for enhancement of their creep resistance. Let us consider the origin of the threshold stresses.

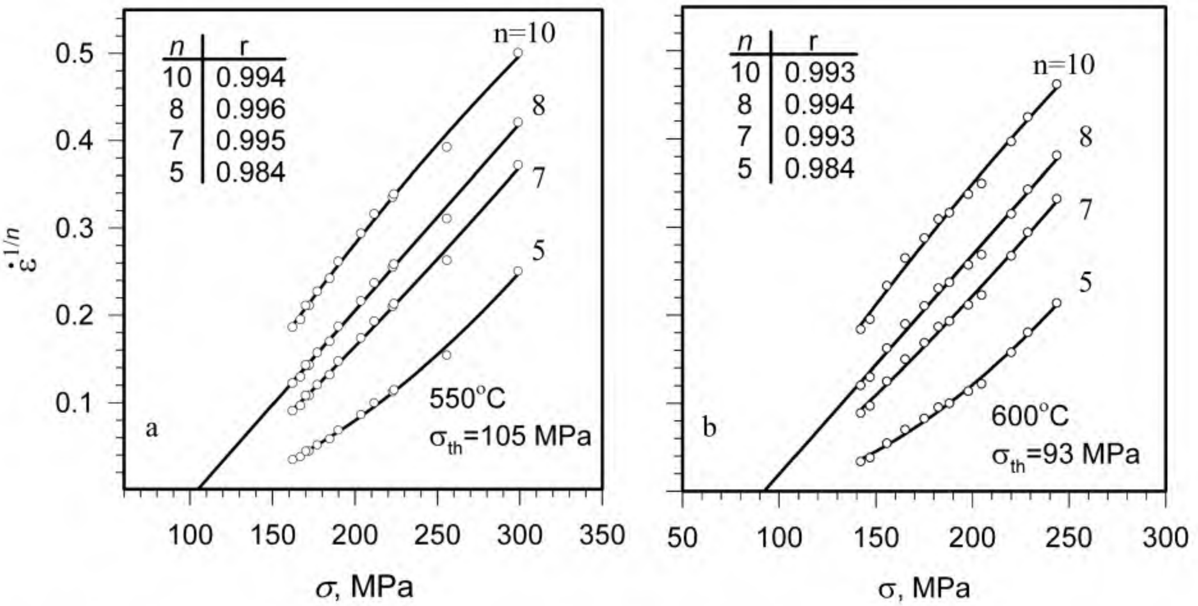

Figure 4. Evaluation of threshold stresses in Fe – 0.6%O steel at 550 and 600°C. The regression coefficients (*r*) of linear approximations for different stress exponents (*n*) are shown in the inserts.

Several theoretical models were developed to evaluate the values of threshold stresses caused by nanoscale dispersoids [10, 12, 13]. Table 1 shows the threshold stresses calculated by using the models of Orowan bowing [12], local climb [13] and detachment [10], taking $d$ = 10 nm, $\lambda$ = 200 nm, $b$ = 0.248 nm and the relaxation parameter $k_d$ = 0.9. The theoretical threshold stresses from local climb and detachment models are quite close to the experimental ones. The TEM observations also suggest that the dislocations overcome the oxide particles by bowing without Orowan loops. The dislocation half-loops can be stable in the case of rather strong attachment interaction between dislocations and particles. Such interaction lowers a free energy because of partial relaxation of long-range elastic stresses from dislocation at interphase boundary. Therefore, the strengthening by dispersed oxides in the studied material is associated with threshold stresses, which are required to detach the moving dislocations from particles.

Table 1. The experimental and theoretical values for threshold stresses [MPa] of the Fe-0.6%O alloy estimated from different models for fine incoherent oxide particles.

| Model | Magnitude of $\sigma_{th}$ | 550°C | 600°C | 650°C | 700°C |
|---|---|---|---|---|---|
| Experimental threshold stress | | 100 | 95 | 90 | 80 |
| Orowan stress [23] | $\sigma_o$=0.84Eb/($\lambda$-d) | 377.3 | 361.1 | 342.6 | 321.7 |
| Local climb [24] | $\sigma_b$=0.3Eb/$\lambda$ | 121.3 | 116.1 | 110.1 | 103.4 |
| Detachment stress[18] | $\sigma_d$=Eb/$\lambda$(1-$k_d^2$)$^{1/2}$ | 127.8 | 122.3 | 116.1 | 109 |

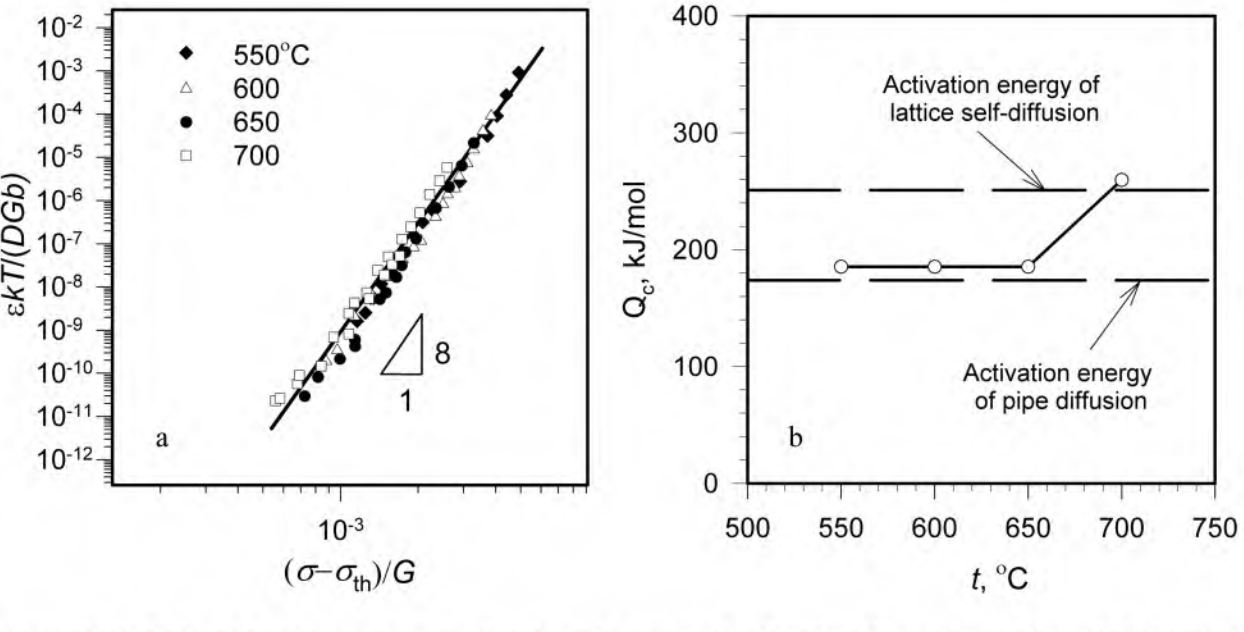

Figure 5. Relationship between normalized strain rate and effective flow stress (a); and deformation activation energy (b) for Fe – 0.6%O steel.

The plot of the normalized strain rate *vs* the normalized effective stress is presented in Fig. 5a. It is clearly seen that all experimental points obey a power law relationship between the strain rate and the normalized effective stresses. The values of deformation activation energies were re-evaluated by using the effective flow stresses $\sigma$-$\sigma_{th}$ (Fig. 5b). The true activation energy of 185 kJ/mol estimated for temperatures of 550 – 650°C is close to the value of activation energy for pipe self-diffusion ($Q_p$ = 174 kJ/mol [5]). An increase in the activation energy to 260 kJ/mol with increase of temperature to 700°C can be associated with transition from the low temperature dislocation climb controlled by pipe-diffusion to the high temperature climb controlled by self-diffusion ($Q_l$=251 kJ/mol).

## Summary

The deformation/creep behavior of Fe – 0.6% O containing nanoscale dispersed oxides with their volume fraction of 2% was studied at temperatures ranging from 550 to 700°C. The dispersed particles acted as effective barriers for dislocation motion and affected significantly the stress – strain rate relationship. The deformation/creep behavior was characterized by a presence of high threshold stresses of about 100 MPa. The dependence of strain rate on effective stress followed a power law relationship with the stress exponent of about 8; and true activation energies of deformation of about 185 and 260 kJ/mol at temperatures of 550-650 and 700 °C, respectively. It is concluded that plastic flow was controlled by pipe diffusion at 550-650°C and lattice diffusion at 700 °C.

## References

[1] Y. Kimura, S. Takaki: Mater. Trans. Vol. 36 (1995), p. 289-296.

[2] Y. Kimura, S. Takaki, S. Suejima, et al.: ISIJ International Vol. 39 (1999), p. 176-182.

[3] A. Belyakov, Y. Sakai, T. Hara, et al.: Metall. Mater. Trans. A. Vol. 33A (2002), p. 3241-3248.

[4] J. Cadek: *Creep in Metallic Materials* (Prague: Academia, 1994).

[5]. H.J. Frost, M.F. Ashby: *Deformation-mechanism maps* (Metallurgiya, 1989).

[6] D.C. Dunand, A.M. Jansen: Acta Mater. Vol. 45 (1997), p. 4569-4581.

[7] J. Čadek, S.J. Zhu, K. Milicka: Mater. Sci. Eng. A. Vol. 252 (1998), p. 1-5.

[8]. D. Haussler, M. Bartsch, U. Messerschmidt, B. Reppich: Acta Mater. Vol. 49 (2001), p. 3647-3657.

[9] A. Wasilkowska, M. Bartsch, U. Messerschmidt: Mater. Proc. Techn. Vol. 133 (2003), p. 218-224.

[10] J. Rosler, E. Arzt: Acta Metall. Vol. 38 (1990), p. 671-683.

[11] K.T. Park, E. Lavernia, F. Mohamed: Acta Metall. Mater. Vol. 42 (1994), p. 667-678.

[12] F. A. Mohamed, K. T. Park, E. J. Lavernia: Mater. Sci. Eng. A. Vol. 150 (1992), p. 21-35.

[13] E. Arzt, D. Wilkinson: Acta Mater. V. 34 (1986), p. 1893-1898.